Penerbit Akademia Baru

Journal of Advanced Research in Micro and Nano Engineering

Journal homepage:
https://www.akademiabaru.com/submit/index.php/armne/index
ISSN: 2756-8210

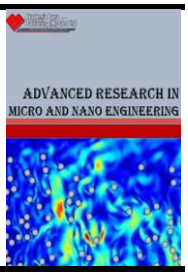

Synthesis of an Ultra-high Hardness Nanostructured AlSi10Mg Alloy via A Hybrid Laser Powder Bed Fusion/High-Pressure Torsion Approach

Shahir Mohd Yusuf[1,*], Nurul Hakimah Lazim[1], Nur Azmah Nordin[1], Saiful Amri Mazlan[1], Nong Gao[2]

[1] Engineering Materials and Structures (eMast) iKohza, Malaysia-Japan International Institute of Technology (MJIIT), UTM Kuala Lumpur, 54100 Kuala Lumpur, Malaysia
[2] Materials Research Group, Mechanical Engineering Department, Faculty of Engineering and Physical Sciences, University of Southampton, Southampton SO17 1BJ, United Kingdom

ARTICLE INFO

Article history:
Received 29 March 2024
Received in revised form 10 May 2024
Accepted 16 June 2024
Available online 30 July 2024

Keywords:
Ultra-high hardness; nanostructured material; AlSi10Mg; hybrid; laser powder bed fusion; high-pressure torsion

ABSTRACT

The hybrid combination of laser powder bed fusion (L-PBF) and high-pressure torsion, respectively an additive manufacturing (AM) and severe plastic deformation (SPD) has recently emerged as an important field of study due to the ability to produce novel nanostructured metals/alloys with simultaneous enhancements in mechanical (hardness, yield and tensile strengths) and functional (corrosion and wear) performances. Pioneering studies on the hybrid L-PBF/HPT approach was focused on 316L stainless steel (316L SS) and AlCuMg alloys due to their widespread engineering applications. AlSi10Mg, an alloy widely used in the automotive industry is expected to benefit from this hybrid combination but has not been investigated before. Thus, this study aims to investigate the microstructural features and hardness of the nanostructured AlSi10Mg attained by the hybrid L-PBF/HPT technique via transmission electron microscopy (TEM) and Vickers microhardness (HV) measurements, respectively. The results showed novel microstructures, including nano-scale grain sizes (< 200 nm), nano-sized Mg_2Si precipitates (~200 nm), and dense dislocation networks. The average hardness value was determined as 230 ± 20 HV, homogeneously distributed throughout the disk surface as indicated by the low deviation (error bar). The microstructures of L-PBF/HPT-synthesised AlSi10Mg are different and significantly refined than conventionally cast AlSi10Mg, which contributed to the two- to four-fold hardness (typical HV values of as-cast AlSi10Mg ranges from 60 – 68 HV) increase via grain boundary and dislocation strengthening mechanisms.

1. Introduction

Laser powder bed fusion (L-PBF) is a well-known additive manufacturing (AM) process that utilizes laser beam as a heat source to selectively melt and fuse successive thin layers (< 100 µm) of powders (feedstock material) to form a complete three-dimensional (3D) object according to its initial computer aided design (CAD) data, among other established AM processes as explained by author from previous studies [1–3]. L-PBF has emerged as a worldwide technological disruptor due to its

* *Corresponding author.*
E-mail address: shahiryasin@utm.my

https://doi.org/10.37934/armne.21.1.6674

capability of fabricating metallic components having complex and/or intricate geometries with high material utilization rate, thereby yielding minimal wastage and thus, low environmental footprint as determined by Abd-Elaziem *et al.,* [4], Furthermore, another key advantage of L-PBF AM process is its ability to fabricate parts made of metals/alloys often comparable or even superior mechanical (e.g. hardness, yield and tensile strengths) and functional (e.g. corrosion and wear) properties compared to conventionally cast/wrought counterparts as discovered by Narasimharaju *et al.,* [5]. Gu *et al.,* [6] explained that such benefits are typically ascribed to the characteristic short laser-material interaction (in the range of ms) and rapid heating/cooling cycles (cooling rates $10^5 – 10^8$ Ks^{-1}) that restrict nucleation and grain growth, thereby yielding unique and novel multi-scale microstructures that include fine grains (1 – 10 µm), ultrafine melt pools comprising of cellular network sub-structures and/or precipitates (< 0.1 µm), and dense dislocation networks (~ 10^{13} m^{-2}). However, L-PBF AM-fabricated parts may be susceptible to porosity due to the pre-existing pores in the raw feedstock powders, as well as anisotropy due to the layer-wise build manner that could diminish the otherwise excellent properties of the attained parts as found out in several previous works [7,8].

On the other hand, high-pressure torsion (HPT) is a forming technique within the family of severe plastic deformation (SPD) processes that impose a combined huge compressive force (1 – 6 GPa) and large amounts of torsional strain (equivalent von Mises strain, ε_{VM-HPT} reaching 136) on bulk metallic materials as described by Wang *et al.,* [9]. Such intense processing approach typically leads to extreme grain refinement down to the nano-scale regime, with large volumes of high-angle grain boundaries (> 60%) possessing average grain sizes < 100 nm, together with nano-dispersoids (10^{-9} m) and denser dislocation networks compared to those attained in L-PBF metallic parts ($10^{14} – 10^{16}$ m^{-2}) as commonly found in various related studies [10–12]. HPT has been applied to cast and wrought metallic parts such as steel, aluminium, copper, and inconel alloys, and has shown significant enhancements in mechanical and functional performances due to the aforementioned microstructural refinements as evidenced by previous studies [9,13]. There is also evidence of HPT processing exhibiting the capability of eliminating porosity in metallic parts due to the immense torsional strains based on the works done by Qi *et al.,* [14]. The similarities in the aspect of microstructural refinement between L-PBF and HPT provide a case for the hybrid combination of these two manufacturing technologies to attain the best advantages of both approaches.

In fact, pioneering studies on the hybrid L-PBF/HPT processing has been conducted by Mohd Yusuf *et al.,* [15–19] on the microstructural and porosity evolution, micromechanical response, strength, corrosion, and tribological performances of 316L SS alloy since 2018. Subsequently, Al Zubaydi *et al.,* [20,21] extended this field of study on AlSiCu alloy by investigating the microstructural and hardness evolutions. In these cases, Mohd Yusuf *et al.,* [19] and Al Zubaydi *et al.,* [20] both found considerable porosity reduction reduction (by ~95%), as well as significant enhancements in strength (by ~2-4 times) for these two hybrid-processed alloys. In addition, Mohd Yusuf *et al.,* [15,18] also discovered enhanced corrosion resistance in (reduction of corrosion rate by ~81%) and tribological performance (reduction of specific wear rate by ~60%) in their study of combining L-PBF and HPT in 316L SS alloy.

Not limiting to these alloys only, it is expected that the hybrid combination of L-PBF/HPT is envisaged to also be advantageous to AlSi10Mg, a common engineering alloy typically used to manufacture automotive components such as engine casing, piston cylinder lining, and brake pads. A nanostructured AlSi10Mg alloy, possessing ultra-high hardness (and thus strength) could potentially be beneficial to enhance the mechanical performance of such automotive parts and further enhance overall service life, especially since they are commonly subjected to numerous loading cycles during operation. Thus, this study aims to produce a nanostructured AlSi10Mg via the

hybrid L-PBF/HPT approach and investigate the microstructural and microhardness evolution through microscopy techniques and Vickers microhardness measurements, respectively. The microstructures and microhardness values are then correlated and compared with those typical of conventionally cast/wrought AlSi10Mg from literature to establish a process-microstructure-property relationship for the material in this study.

2. Methodology

In this study, AlSI10Mg powders with spherical morphology and particle sizes between 0 – 45 µm obtained from MSE Supplies, USA were used as the feedstock material for L-PBF AM. Energy dispersive x-ray spectroscopy (EDX) analysis revealed the following chemical composition of the AlSi10Mg powders (in wt.%): Si: 10.8, Mg: 0.45, Cu: 0.05, Mn: 0.45, Fe: 0.55, Ni: 0.05, Zn: 0.1, Pb: 0.05, Sn: 0.05, Ti: 0.15, and Al: *bal*. Spherical disks with thickness 1 mm and diameter 10 mm (Figure 1(a)) were fabricated by using Concept Laser M2 SLM machine inside an enclosed chamber purged with N_2 gas at room temperature using the following processing parameters: laser power, *P*: 400 W, scan speed, *v*: 1600 mm s^{-1}, laser scan spacing, *h*: 200 µm, layer thickness, *d*: 20 µm, and an alternating bi-directional scan strategy based on the works of Yusuf *et al.,* [22]. The disks were fabricated with the circular cross-section being parallel to the build surface (Figure 1(b)). The dimensions of the specimens to be fabricated by L-PBF were chosen based on those that could fit inside the HPT processing machine.

The disks were then subjected to HPT processing in a HPT facility at room temperature. The disks were placed inside circular depressions one each at the lower and upper anvils of the machine. The lower anvil was pushed upwards to provide compressive force, followed by its rotation for 10 revolutions to impose torsional straining under 6 GPa pressure at 1 rpm. The equivalent von mises strain, ε_{VM} can be estimated based on the following equation described by Edalati *et al.,* [23]

$$\mathcal{E}_{VM-HPT} = \frac{2\pi N R}{h\sqrt{3}} \quad (1)$$

where *N* is the number of HPT revolutions (*N*=10 in this study), *R* is the distance from the centre, and *h* is the initial disk thickness. Based on Eq. (1), the HPT-imposed ε_{VM} value was evaluated as 136. The overall dimensions of specimens to be fabricated and the HPT equipment setup are shown in Figure 1 based on the previous work of Zhang *et al.,* [24].

The hybrid manufactured specimens were then subjected to sample preparation procedures for transmission electron microscopy (TEM) detailed in the work of Mohd Yusuf *et al.,* in Ref. [16]. Microstructural features such as grains, precipitates, and dislocations were revealed via this microscopy technique. In particular, the grain sizes were measured by using the method described by Thorvaldsen [25] via evaluation of at least 300 grains through ≥ 20 TEM images taken at the peripheral disk regions (3.5 mm from the centre). Subsequently, the average Vickers microhardness (HV) value was obtained by HV measurements taken at 100 different locations throughout the peripheral regions of each disk, 3.5 mm from the disk centre using an applied load of 500 gf under a 15 s dwell time. The HV measurements were repeated on 10 disks to improve statistical accuracy.

The microstructures and microhardness of the nanostructured AlSi10Mg attained via the hybrid L-PBF/HPT approach in this study were correlated to establish a process-microstructure-property relationship, and also compared with the typical corresponding features and values of conventionally cast AlSi10Mg alloy, respectively from existing literature.

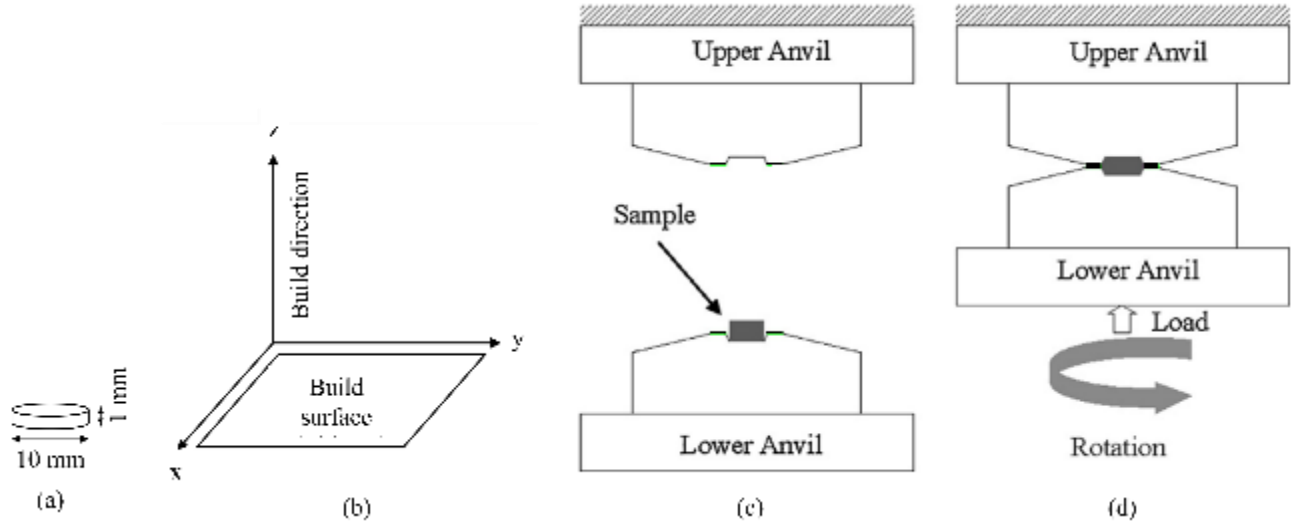

Fig. 1. (a) Dimensions of specimens to be fabricated, (b) build surface and direction of the L-PBF process. Schematic of (c) HPT machine setup and (d) process based on the works of Zhang *et al.,* [24]

3. Results and discussions

3.1 Microstructural Features

Figure 2 shows representative TEM images of the hybrid L-PBF/HPT-synthesised AlSi10Mg specimens. It is evident that the extreme grain refinement yielded a nanostructured material with nano-scale grain sizes of < 200 nm (dark field (DF) TEM image in Figure 2(a)). Meanwhile, the red circles shown in the bright field (BF) TEM image of Figure 2(b) exhibits examples of nano-scale grains that contain dense dislocation networks within their interior, which indicate non-equilibrium grain boundaries (GBs) typical of HPT processing, as suggested by Sauvage *et al.,* [26]. Additionally, Figure 2(b) also displays grains without any internal structures, which suggest competing grain refinement and dislocation nucleation/annihilation mechanisms resulting from plastic shearing induced by the extreme HPT torsional straining as explained in numerous studies [27–30]. Nevertheless, such microstructures have been found to similarly provide strengthening to the nanostructured metals/alloys by becoming direct sites of dislocation motion impediment based on evidences from established studies [28,31]. Furthermore, the high-angle annular dark field (HAADF) TEM image of Figure 2(c) depicts examples of nano-sized Mg_2Si precipitates (~200 nm) that were refined during the hybrid L-PBF/HPT process. The presence of such nano-precipitates is confirmed by the elemental area maps shown in Figures 2(d)-(f) obtained through energy dispersive x-ray spectroscopy (EDX) analysis apparatus equipped with the TEM facility.

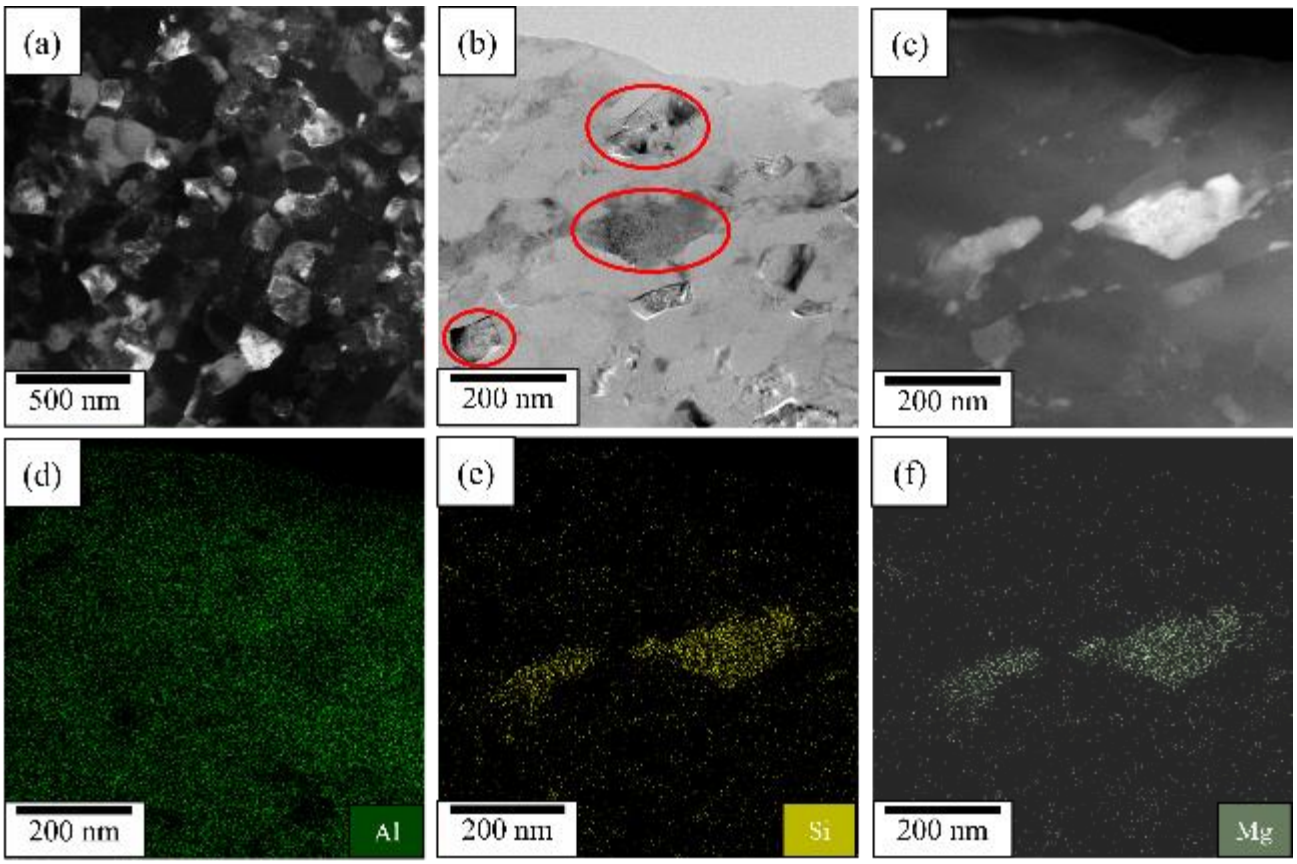

Fig. 2. TEM images of hybrid L-PBF/HPT-processed AlSi10Mg

On the other hand, Figure 3 depicts typical microstructures of as-cast AlSi10Mg that consist of dendritic structures (Figure 3(a)) comprising of coarse α-Al matrix, fine needle-like Al-Si eutectic structures (Figure 3(b)), Mg_2Si precipitates (Figure 3(c)), and dislocations (Figure 3(d)) as obtained by Snopiński *et al.,* [32] in their study on the microstructures and mechanical properties of cast vs. L-PBF AM-fabricated AlSi10Mg. These microstructures are clearly different that those attained via the hybrid L-PBF/HPT technique shown in Figure 2. In particular, the overall microstructures are much coarser than the hybrid L-PBF/HPT-manufactured part, which can be ascribed to the low cooling rates experienced during casting (up to 10^{10} Ks^{-1} only) that promotes nucleation and grain growth, as observed by Samantaray *et al.,* [33]. Vice versa, the significantly finer microstructures of the L-PBF/HPT part can be attributed to the combined high cooling rates of L-PBF AM (10^5 – 10^8 Ks^{-1}) and extreme torsional straining of HPT process, which not only restricts grain growth and produces fine microstructures (L-PBF), but also refines those microstructures to the nano-scale region, as explained in previous works [16,34]. Furthermore, although not evaluated in the present study, the dislocation density of the nanostructured AlSi10Mg is expected to be in the range of 10^{14} – 10^{16} m^{-2}, as has been found in numerous related studies [10–12], significantly higher than 10^9 – 10^{10} m^{-2} typically obtained in cast metals/alloys [35]. Qualitatively, such difference in dislocation densities can be observed in Figure 2(a) for the hybrid L-PBF/HPT AlSi10Mg and Figure 3(d) for the cast counterpart. It is clear that the dislocation density of the former is significantly denser and forms a network compared to the less-dense dislocations that are characterised by thin individual strands of the latter. The formation of dense dislocation networks is commonly attributed to the generation and multiplication of dislocations due to the shear strain induced by HPT according to the strain gradient plasticity theory explained by Ashby [36].

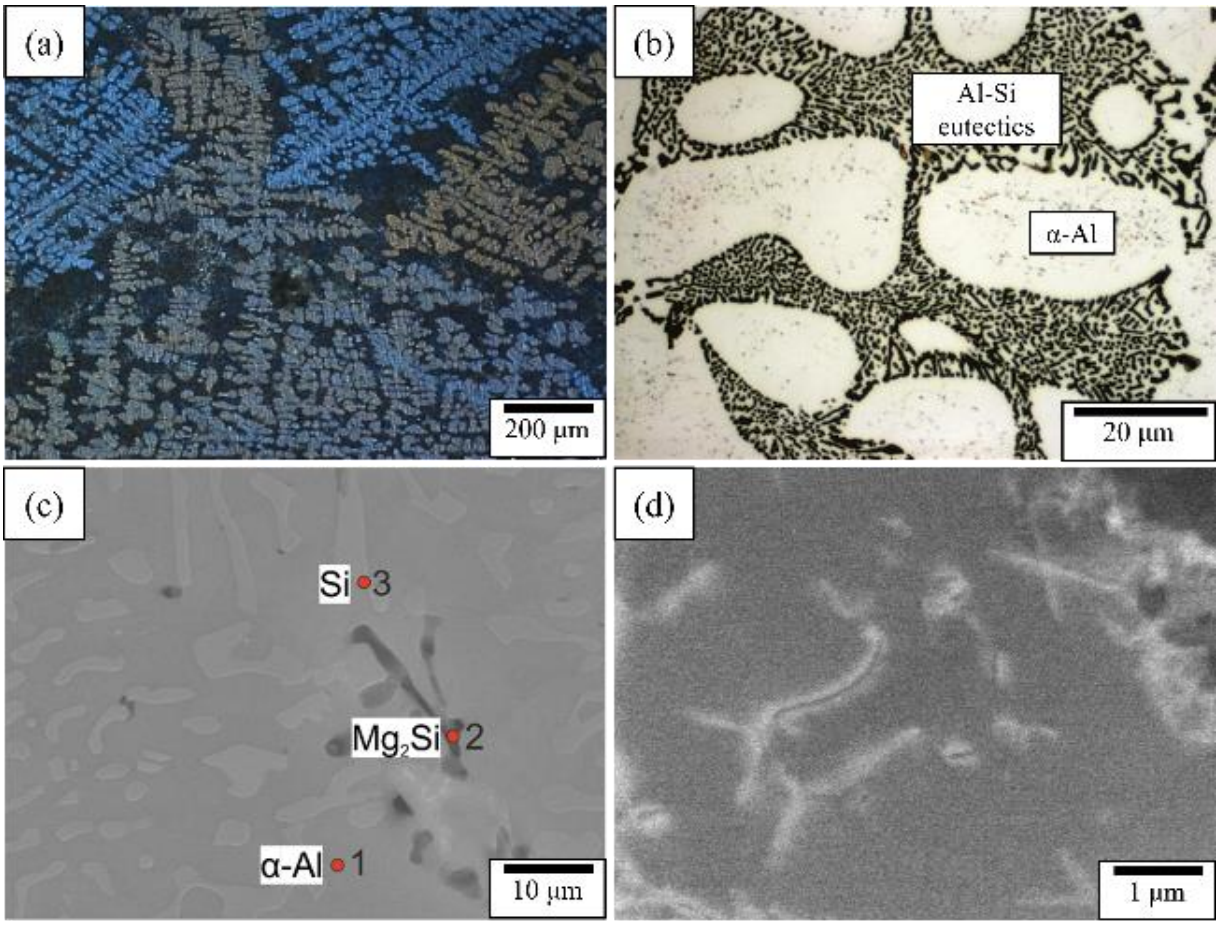

Fig. 3. Typical microstructures of as-cast AlSi10Mg based on the works of Snopiński *et al.,* [32]

3.2 Hardness

The average Vickers microhardness value of the nanostructured AlSi10Mg synthesised through the hybrid L-PBF/HPT technique in this study was determined as 230 ± 20 HV, which is considerably higher than ~60 – 80 HV typically obtained for cast AlSi10Mg (~2 – 4-fold increase) in various studies [32,37,38]. The significantly high hardness can be associated with the contributions by the nano-scale grains through grain boundary strengthening and dense dislocation networks via dislocation strengthening, which are common for HPT-processed metals and alloys, as determined in previous related investigations [16,20,39]. Actually, there is another possible strengthening mechanism that could contribute to the high hardness in this study through precipitation strengthening via Orowan shearing and/or looping/bypass mechanism, i.e. dislocations cutting/shearing through the precipitates and/or dislocations bypassing/looping through the precipitates, as discovered by Chen *et al.,* [40]. However, there are no evidences that can discern such occurrence, even by TEM in the present investigation. Thus, it can be reasonably inferred that no precipitation strengthening mechanism is exhibited, and the L-PBF/HPT-fabricated AlSi10Mg is only strengthened by the grain boundary and dislocation strengthening mechanisms. On the other hand, despite the extensive microhardness measurements (100 measurements throughout the peripheral regions of each disk for 10 disks), the deviation of the HV values can be considered to be in the low range, varying from 210 to 240 HV. This is an interesting observation because Eq. (1) estimates a radial dependency in terms of the ε_{VM-HPT} values in terms of the HPT-imposed shear strain distribution. Based on the equation, lower strains should be experienced at the central disk areas (0 – 2.5 mm from the centre) compared to the peripheral disk areas (> 2.5 mm from the centre), thereby suggesting higher HV

values at the peripheral compared to the central area. However, the small deviation in HV values in the current study suggests similar hardness, and thus homogeneous hardness distribution throughout the disk surface. This phenomenon is commonly termed 'strain saturation' that describes the decreasing rate of work hardening until a critical torsional strain level is reached commonly observed in previous works [41–43] (ε_{VM}= 136 from 10 HPT revolutions in this study).

4. Conclusions

In the present study, a nanostructured AlSi10Mg alloy was successfully synthesised by a hybrid L-PBF/HPT approach, followed by microstructural characterisation via TEM and hardness testing through Vickers microhardness (HV) measurements. The following conclusions can be drawn based on the results of this study:

i. Nano-scale grains (< 200 nm), nano-sized Mg_2Si precipitates, and dense dislocation networks were attained, which are significantly different from conventionally cast AlSi10Mg.
ii. Two- to four-fold hardness increase in HV values were observed compared to conventionally cast AlSi10Mg.
iii. The low deviation in HV values suggests homogeneous hardness distribution throughout the disk surface.
iv. The significant increase in hardness of the nanostructured AlSi10Mg attained by the hybrid L-PBF/HPT technique can be ascribed to the combination of grain boundary and dislocation strengthening mechanisms.

Acknowledgement
This work was funded by the Ministry of Higher Education (MOHE) Malaysia under the Fundamental Research Grant Scheme (FRGS /1/2021/TK0/UTM/02/84).

References
[1] Baharudin, Mohamad Ezral, Mohd Sazli Saad, Mohd Zakimi Zakaria, Azuwir Mohd Nor, and Mat Hussin Ab Talib. "FDM Parameters Optimization for Improving Tensile Strength using Response Surface Methodology and Particle Swarm Optimization." *Journal of Advanced Research in Applied Sciences and Engineering Technology* 38, no. 2 (2024): 112-128. https://doi.org/10.37934/araset.38.2.112128
[2] Alias, Nur Nazira, Ireana Yusra Abdul Fatah, Yew Been Seok, Sharifah Hanis Yasmin Sayid Abdullah, Amir Hussain Bhat, and Saiful Bahri Mohd Diah. "Material Characterizations of the Polymers Reinforced with Recycled Flexible Plastic Blends as Filament for 3D Printing." *Journal of Advanced Research in Applied Sciences and Engineering Technology* 37, no. 1 (2024): 1-15. https://doi.org/10.37934/araset.37.1.115
[3] Hidayah Musa, Nur, Nurainaa Mazlan, Shahir Mohd Yusuf, Nur Azmah Nordin, Saiful Amri Mazlan, and Nong Gao. "High densification level and hardness values of additively manufactured 316L stainless steel fabricated by fused filament fabrication." *Journal of Advanced Research in Applied Sciences and Engineering Technology* 34, no. 2 (2023): 144-152. https://doi.org/10.37934/araset.34.2.144152
[4] Abd-Elaziem, Walaa, Sally Elkatatny, Abd-Elrahim Abd-Elaziem, Mahmoud Khedr, Marwa A. Abd El-baky, Mohamed Ali Hassan, Mohamed Abu-Okail et al. "On the current research progress of metallic materials fabricated by laser powder bed fusion process: a review." *Journal of Materials Research and Technology* 20 (2022): 681-707. https://doi.org/10.1016/j.jmrt.2022.07.085
[5] Narasimharaju, Shubhavardhan Ramadurga, Wenhan Zeng, Tian Long See, Zicheng Zhu, Paul Scott, Xiangqian Jiang, and Shan Lou. "A comprehensive review on laser powder bed fusion of steels: Processing, microstructure, defects and control methods, mechanical properties, current challenges and future trends." *Journal of Manufacturing Processes* 75 (2022): 375-414. https://doi.org/10.1016/j.jmapro.2021.12.033
[6] Gu, Dong Dong, Wilhelm Meiners, Konrad Wissenbach, and Reinhart Poprawe. "Laser additive manufacturing of metallic components: materials, processes and mechanisms." *International materials reviews* 57, no. 3 (2012): 133-164. https://doi.org/10.1179/1743280411Y.0000000014

[7] Lewandowski, John J., and Mohsen Seifi. "Metal additive manufacturing: a review of mechanical properties." *Annual review of materials research* 46, no. 1 (2016): 151-186. https://doi.org/10.1146/annurev-matsci-070115-032024

[8] DebRoy, Tarasankar, Huiliang L. Wei, James S. Zuback, Tuhin Mukherjee, John W. Elmer, John O. Milewski, Allison Michelle Beese, A. de Wilson-Heid, Amitava De, and Wei Zhang. "Additive manufacturing of metallic components–process, structure and properties." *Progress in materials science* 92 (2018): 112-224. https://doi.org/10.1016/j.pmatsci.2017.10.001

[9] Wang, Zhi-Rui, Ping-Zhan Si, Jihoon Park, Chul-Jin Choi, and Hong-Liang Ge. "A review of ultrafine-grained magnetic materials prepared by using high-pressure torsion method." *Materials* 15, no. 6 (2022): 2129. https://doi.org/10.3390/ma15062129

[10] Li, Zhuoliang, Hua Ding, Yi Huang, and Terence G. Langdon. "An Evaluation of the Mechanical Properties, Microstructures, and Strengthening Mechanisms of Pure Mg Processed by High-Pressure Torsion at Different Temperatures." *Advanced Engineering Materials* 24, no. 10 (2022): 2200799. https://doi.org/10.1002/adem.202200799

[11] Gubicza, Jenő, Anita Heczel, Megumi Kawasaki, Jae-Kyung Han, Yakai Zhao, Yunfei Xue, Shuo Huang, and János L. Lábár. "Evolution of microstructure and hardness in Hf25Nb25Ti25Zr25 high-entropy alloy during high-pressure torsion." *Journal of Alloys and Compounds* 788 (2019): 318-328. https://doi.org/10.1016/j.jallcom.2019.02.220

[12] Khaleghi, A. A., F. Akbaripanah, M. Sabbaghian, K. Máthis, P. Minárik, J. Veselý, M. El-Tahawy, and J. Gubicza. "Influence of high-pressure torsion on microstructure, hardness and shear strength of AM60 magnesium alloy." *Materials Science and Engineering: A* 799 (2021): 140158. https://doi.org/10.1016/j.msea.2020.140158

[13] Azzeddine, Hiba, Djamel Bradai, Thierry Baudin, and Terence G. Langdon. "Texture evolution in high-pressure torsion processing." *Progress in Materials Science* 125 (2022): 100886. https://doi.org/10.1016/j.pmatsci.2021.100886

[14] Qi, Yuanshen, Anna Kosinova, Askar R. Kilmametov, Boris B. Straumal, and Eugen Rabkin. "Generation and healing of porosity in high purity copper by high-pressure torsion." *Materials Characterization* 145 (2018): 1-9. https://doi.org/10.1016/j.matchar.2018.08.023

[15] Yusuf, Shahir Mohd, Mengyan Nie, Ying Chen, Shoufeng Yang, and Nong Gao. "Microstructure and corrosion performance of 316L stainless steel fabricated by Selective Laser Melting and processed through high-pressure torsion." *Journal of Alloys and Compounds* 763 (2018): 360-375. https://doi.org/10.1016/j.jallcom.2018.05.284

[16] Yusuf, Shahir Mohd, Ying Chen, Shoufeng Yang, and Nong Gao. "Microstructural evolution and strengthening of selective laser melted 316L stainless steel processed by high-pressure torsion." *Materials Characterization* 159 (2020): 110012. https://doi.org/10.1016/j.matchar.2019.110012

[17] Mohd Yusuf, Shahir, Ying Chen, Shoufeng Yang, and Nong Gao. "Micromechanical Response of Additively Manufactured 316L Stainless Steel Processed by High-Pressure Torsion." *Advanced Engineering Materials* 22, no. 10 (2020): 2000052. https://doi.org/10.1002/adem.202000052

[18] Yusuf, Shahir Mohd, Daryl Lim, Ying Chen, Shoufeng Yang, and Nong Gao. "Tribological behaviour of 316L stainless steel additively manufactured by laser powder bed fusion and processed via high-pressure torsion." *Journal of Materials Processing Technology* 290 (2021): 116985. https://doi.org/10.1016/j.jmatprotec.2020.116985

[19] Mohd Yusuf, Shahir, Ying Chen, Nur Hidayah Musa, Nurainaa Mazlan, Nur Azmah Nordin, Nurhazimah Nazmi, Saiful Amri Mazlan, and Nong Gao. "Elimination of porosity in additively manufactured 316L stainless steel by high-pressure torsion." *The International Journal of Advanced Manufacturing Technology* 123, no. 3 (2022): 1175-1187. https://doi.org/10.1007/s00170-022-10228-w

[20] Al-Zubaydi, Ahmed SJ, Nong Gao, Shuncai Wang, and Philippa AS Reed. "Microstructural and hardness evolution of additively manufactured Al–Si–Cu alloy processed by high-pressure torsion." *Journal of Materials Science* 57, no. 19 (2022): 8956-8977. https://doi.org/10.1007/s10853-022-07234-4

[21] Al-Zubaydi, Ahmed SJ, Nong Gao, Jan Dzugan, Pavel Podany, Sandeep Sahu, Deepak Kumar, Ying Chen, and Philippa AS Reed. "The hot deformation behaviour of laser powder bed fusion deposited Al–Si–Cu alloy processed by high-pressure torsion." *Journal of Materials Science* 57, no. 43 (2022): 20402-20418. https://doi.org/10.1007/s10853-022-07847-9

[22] Yusuf, Shahir Mohd, Mathias Hoegden, and Nong Gao. "Effect of sample orientation on the microstructure and microhardness of additively manufactured AlSi10Mg processed by high-pressure torsion." *The International Journal of Advanced Manufacturing Technology* 106 (2020): 4321-4337. https://doi.org/10.1007/s00170-019-04817-5

[23] Edalati, Kaveh, and Zenji Horita. "A review on high-pressure torsion (HPT) from 1935 to 1988." *Materials Science and Engineering: A* 652 (2016): 325-352. https://doi.org/10.1016/j.msea.2015.11.074

[24] Zhang, Jiuwen, Nong Gao, and Marco J. Starink. "Al–Mg–Cu based alloys and pure Al processed by high pressure torsion: The influence of alloying additions on strengthening." *Materials Science and Engineering: A* 527, no. 15 (2010): 3472-3479. https://doi.org/10.1016/j.msea.2010.02.016

[25] Thorvaldsen, A. "The intercept method—1. Evaluation of grain shape." *Acta materialia* 45, no. 2 (1997): 587-594. https://doi.org/10.1016/S1359-6454(96)00197-8
[26] Sauvage, Xavier, Gerhard Wilde, S. V. Divinski, Zenji Horita, and R. Z. Valiev. "Grain boundaries in ultrafine grained materials processed by severe plastic deformation and related phenomena." *Materials Science and Engineering: A* 540 (2012): 1-12. https://doi.org/10.1016/j.msea.2012.01.080
[27] Scheriau, Stephan, and Reinhard Pippan. "Influence of grain size on orientation changes during plastic deformation." *Materials Science and Engineering: A* 493, no. 1-2 (2008): 48-52. https://doi.org/10.1016/j.msea.2007.08.092
[28] Scheriau, S., Zaoli Zhang, S. Kleber, and Reinhard Pippan. "Deformation mechanisms of a modified 316L austenitic steel subjected to high pressure torsion." *Materials Science and Engineering: A* 528, no. 6 (2011): 2776-2786. https://doi.org/10.1016/j.msea.2010.12.023
[29] Vorhauer, Andreas, and Reinhard Pippan. "On the homogeneity of deformation by high pressure torsion." *Scripta Materialia* 51, no. 9 (2004): 921-925. https://doi.org/10.1016/j.scriptamat.2004.04.025
[30] Pippan, Reinhard, Florian Wetscher, Martin Hafok, Andreas Vorhauer, and Ishaf Sabirov. "The limits of refinement by severe plastic deformation." *Advanced Engineering Materials* 8, no. 11 (2006): 1046-1056. https://doi.org/10.1002/adem.200600133
[31] Wu, Wenqian, Min Song, Song Ni, Jingshi Wang, Yong Liu, Bin Liu, and Xiaozhou Liao. "Dual mechanisms of grain refinement in a FeCoCrNi high-entropy alloy processed by high-pressure torsion." *Scientific reports* 7, no. 1 (2017): 46720. https://doi.org/10.1038/srep46720
[32] Snopiński, Przemysław, Mariusz Król, Marek Pagáč, Jana Petrů, Jiří Hajnyš, Tomasz Mikuszewski, and Tomasz Tański. "Effects of equal channel angular pressing and heat treatments on the microstructures and mechanical properties of selective laser melted and cast AlSi10Mg alloys." *Archives of Civil and Mechanical Engineering* 21, no. 3 (2021): 92. https://doi.org/10.1007/s43452-021-00246-y
[33] Samantaray, Dipti, Vinod Kumar, A. K. Bhaduri, and Pradip Dutta. "Microstructural evolution and mechanical properties of type 304 L stainless steel processed in semi-solid state." *international journal of metallurgical engineering* 2, no. 2 (2013): 149-153.
[34] Saeidi, Kamran, X. Gao, Yuan Zhong, and Zhijian James Shen. "Hardened austenite steel with columnar sub-grain structure formed by laser melting." *Materials Science and Engineering: A* 625 (2015): 221-229. https://doi.org/10.1016/j.msea.2014.12.018
[35] Pham, M. S., B. Dovgyy, and P. A. Hooper. "Twinning induced plasticity in austenitic stainless steel 316L made by additive manufacturing." *Materials Science and Engineering: A* 704 (2017): 102-111. https://doi.org/10.1016/j.msea.2017.07.082
[36] Ashby, M. F. "The deformation of plastically non-homogeneous materials." *The Philosophical Magazine: A Journal of Theoretical Experimental and Applied Physics* 21, no. 170 (1970): 399-424. https://doi.org/10.1080/14786437008238426
[37] Shakil, S. I., A. Hadadzadeh, B. Shalchi Amirkhiz, H. Pirgazi, M. Mohammadi, and M. Haghshenas. "Additive manufactured versus cast AlSi10Mg alloy: Microstructure and micromechanics." *Results in Materials* 10 (2021): 100178. https://doi.org/10.1016/j.rinma.2021.100178
[38] Van Cauwenbergh, P., V. Samaee, L. Thijs, J. Nejezchlebová, P. Sedlák, A. Iveković, D. Schryvers, B. Van Hooreweder, and K. Vanmeensel. "Unravelling the multi-scale structure–property relationship of laser powder bed fusion processed and heat-treated AlSi10Mg." *Scientific reports* 11, no. 1 (2021): 6423. https://doi.org/10.1038/s41598-021-85047-2
[39] Mavlyutov, Aydar, Alexey Evstifeev, Darya Volosevich, Marina Gushchina, Artem Voropaev, Oleg Zotov, and Olga Klimova-Korsmik. "The Effect of Severe Plastic Deformation on the Microstructure and Mechanical Properties of Composite from 5056 and 1580 Aluminum Alloys Produced with Wire Arc Additive Manufacturing." *Metals* 13, no. 7 (2023): 1281. https://doi.org/10.3390/met13071281
[40] Chen, B., S. K. Moon, X. Yao, G. Bi, J. Shen, J. Umeda, and K. Kondoh. "Strength and strain hardening of a selective laser melted AlSi10Mg alloy." *Scripta Materialia* 141 (2017): 45-49. https://doi.org/10.1016/j.scriptamat.2017.07.025
[41] Kawasaki, Megumi, Roberto B. Figueiredo, and Terence G. Langdon. "An investigation of hardness homogeneity throughout disks processed by high-pressure torsion." *Acta Materialia* 59, no. 1 (2011): 308-316. https://doi.org/10.1016/j.actamat.2010.09.034
[42] Kawasaki, Megumi. "Different models of hardness evolution in ultrafine-grained materials processed by high-pressure torsion." *Journal of Materials Science* 49 (2014): 18-34. https://doi.org/10.1007/s10853-013-7687-9
[43] Kawasaki, Megumi. "Different models of hardness evolution in ultrafine-grained materials processed by high-pressure torsion." *Journal of Materials Science* 49 (2014): 18-34. https://doi.org/10.1007/s10853-013-7687-9